Electron spectroscopy on boron nitride thin films: Comparison of near-surface to bulk electronic properties

P. Widmayer, H.-G. Boyen, and P. Ziemann
Abteilung Festkörperphysik, Universität Ulm, D-89069 Ulm, Germany

P. Reinke and P. Oelhafen
Institut für Physik, Universität Basel, Klingelbergstrasse 82, CH-4056 Basel, Switzerland
(Received 1 June 1998; revised manuscript received 17 September 1998)

Combining spectroscopic methods probing both occupied as well as unoccupied electronic states, the surface electronic structure of *ex situ* prepared boron-nitride films is analyzed and compared to experimental and theoretical bulk-electronic properties taken from the literature. X-ray photoelectron spectroscopy is applied to probe the core-level and valence-band electronic states, electron-energy-loss spectroscopy in the reflection geometry to investigate conduction band states as well as excitations like plasmons and core excitons. For films with hexagonal structure, the results from the near-surface region are found to reflect both the ground state and the many-body properties of the bulk material. Cubic boron nitride films in all cases exhibit a hexagonal-like top layer with a thickness of about 0.9 nm. Low-energy ion bombardment at room temperature is found to significantly increase the amount of disorder in both types of films, leading to the transformation of the cubic phase into a hexagonal-like material. [S0163-1829(99)02607-7]

I. INTRODUCTION

Boron nitride is a material that has attracted continuous interest for more than three decades. Like carbon, boron nitride forms a variety of atomic structures of which the hexagonal and the cubic phase, in particular, have been the subject of extensive theoretical and experimental work. Hexagonal boron nitride (h-BN), a sp^2-bonded layered-compound isostructural to graphite, exhibits strong anisotropic physical properties. Its electronic structure, though sharing many similarities with graphite, however, leads to a wide-gap semiconducting behavior in contrast to the semimetallic nature of graphite. Due to its high thermal stability h-BN is a widely used material in vacuum technology. In addition, it has been employed for microelectronic devices,[1] for x-ray lithography masks,[2] and as a wear-resistant lubricant.[3]

The cubic phase of boron nitride (c-BN), on the other hand, has the zinc-blende lattice structure with sp^3-hybridized B-N bonds. It is the second-hardest material known after diamond, with even better properties for a wide range of applications. Among them, c-BN does not react with ferrous materials even at temperatures as high as 1600 K.[4] In contrast to diamond, c-BN can be doped to form both n-type as well as p-type semiconductors, which becomes increasingly important in semiconductor device industry in order to produce high-temperature microelectronic systems. Recently, a negative-electron affinity has been reported for bulk material and thin films, promising cold-cathode electron emitters with stable properties.[5,6]

Since there is considerable interest in boron nitride due to its technological importance, extensive theoretical[7–25] and experimental work has been devoted to the electronic properties of this material. Many methods have been employed to explore the electronic structure of boron nitride, among which are methods like soft-x-ray emission spectroscopy[26–35] and photoelectron spectroscopy,[27,36–41] which are both sensitive to occupied electronic states, as well as near-edge x-ray absorption fine structure spectroscopy[26,42–49] (NEXAFS) and energy-loss near-edge spectroscopy (ELNES),[50,51] which can be used to probe the unoccupied part of the band structure. In addition, electron-energy-loss spectroscopy performed in the plasmon region has proved to provide valuable information.[50,52–58]

Despite all the theoretical and experimental efforts, deviations from band-structure calculations are evident in many studies concerning the width of the energy gap, the widths of the energy bands, and the energy positions of characteristic features in the density of states, respectively.[20,34,36,39,53] Very often, the energy scales of calculated data have been adjusted to match experimental results. On the other hand, conflicting experimental data have been reported, resulting from difficulties in the energy calibration.[34,49]

While, in general, there is reasonable agreement between theory and experiments for carbon-based systems, this is not the case for boron nitride. The reason for this may partially be due to problems in the preparation of large ($>$0.3 mm) single-crystalline samples providing well-defined surfaces, which has been achieved only very recently.[59] While most of the above studies were performed on polycrystalline bulk materials prepared at high temperatures and high pressures, thin films and coatings, which are the most promising candidates for future applications, are even less understood. Thin films are commonly processed under nonequilibrium conditions resulting in nanocrystalline materials.[4,60,61] This leads to a large scatter in the experimentally observed electronic properties among different samples, as can be seen by, e.g., reported plasmon energies for c-BN films ranging from 28 to 32 eV.[50,57,58] Whereas, for bulk samples, clean surfaces can be achieved by methods like scraping or cleaving, such is not possible for *ex situ* prepared thin films, making contaminations a serious problem for most of the surface-sensitive methods. Another reason for contradictive experimental results may be connected to a nonhomogeneous structure

TABLE I. Film composition x and amount of dominant contaminants as determined by XPS.

Sample	B_xN_{100-x}	Oxygen (at. %)	Carbon (at. %)
h-BN (annealed to 520 K)	51.0	3.5	4.6
h-BN (irradiated with 5 keV Ar^+)	52.6	2.0	<1
c-BN (annealed to 520 K)	50.1	8.3	7.3
c-BN (irradiated with 5 keV Ar^+)	54.2	2.7	1.7

within the sampling depth of the technique used to characterize the electronic states.[57,62,63] Finally, the commonly applied ion etching procedures performed for surface cleaning or depth profiling may lead to artificial results due to uncontrolled changes of the stoichiometry and microstructure of the irradiated region.

Until now it was an open question whether boron nitride thin films can reliably be characterized by means of *surface* sensitive techniques. It is the aim of the present paper to answer this question by demonstrating that the volume electronic properties of boron nitride thin films can be determined applying surface-sensitive spectroscopic tools. We will show that the combination of x-ray photoelectron spectroscopy (XPS) on core level as well as valence states with electron-energy-loss spectroscopy in the reflection geometry (REELS) allows us to achieve a consistent picture of the surface-electronic structure of thin films. While, in the case of h-BN the results reflect the properties of bulk material, this is not the case for c-BN films due to the existence of a top layer with a hexagonal-like structure, whose thickness can be determined to be 0.9 nm. Emphasis is put on a thorough characterization of the films with respect to their chemical state, stoichiometry, and the level of possible contamination.

II. EXPERIMENTAL DETAILS

The BN thin films studied in this paper were prepared onto Si(100) substrates at a temperature of 670 K by an ion-beam-assisted sputter-deposition process using two Kaufman ion sources. Elemental boron (99.9%) was sputter eroded using 1.5 keV Ar^+ ions, while the growing film was simultaneously irradiated with a mixture of argon and nitrogen ions. Hexagonal films were deposited using pure nitrogen as assisting ion beam. For more details, see Ref. 64. Applying transmission infrared spectroscopy, the integral c-BN content of the films was determined from the peak height ratio of the c-BN TO mode and the h-BN in-plane mode, respectively. With this procedure, the volume fraction of the cubic phase of the studied c-BN samples with thicknesses ranging from 80 to 100 nm was found to be larger than 70%. Following the widely accepted model of a layered growth,[63–65] the by-far largest contribution to the h-BN infrared signals originates from the h-BN nucleation layer. Even if h-BN grain boundaries[66] are taken into account, it is justified to consider the upper part of the c-BN films to predominantly consist of the pure cubic phase.

Electron spectroscopy was performed at a pressure of 1×10^{-10} mbar in a FISONS ESCALAB-210 electron spectrometer, which is equipped with a small spot x-ray source and an electron gun allowing primary energies E_0 up to 3 keV. Monochromatized Al $K\alpha$ radiation ($h\nu=1486.6$ eV) was exploited to perform a chemical analysis of the sample surface and to investigate the details of the valence-band structure. In order to calibrate the instrument, the Fermi edge of an Au reference sample has been measured, which can be used to define the origin of the binding-energy scale ($E_B=0$) in the conventional manner. REELS measurements were done to study the energy-loss function in the plasmon-energy range (0–50 eV) and at the B 1s absorption edge (185–240 eV), allowing to characterize the unoccupied density of states at the boron sites. The total energy resolution in the photoemission experiments was adjusted to a value of 0.7 eV (full width at half maximum). In the REELS measurements, the total energy resolution was between 0.7 eV ($E_0=350$ eV) and 1.3 eV ($E_0=2.5$ keV), mainly caused by the broadening of the primary electron beam. In order to reduce the surface contaminations as much as possible, all samples were carefully outgassed prior to the spectroscopic measurements at a temperature of 520 K,[49] which is well below the temperature during growth (670 K). In order to study the influence of disorder, an additional irradiation was performed with low-energy Ar^+ ions.

In Table I, the results of the chemical analysis are summarized for the outgassed as well as the irradiated films. These data are obtained from core-level spectra of the B 1s, N 1s, C 1s, and O 1s lines, whose relative intensities are determined by means of a numerical-fitting procedure[67] and using the corresponding photoionization cross sections as given in Ref. 68. As can be judged from Table I, the spectroscopic information sampled over a depth of 4–5 nm allows us to conclude that the various as-prepared BN films are stoichiometric. Even after the annealing step, a significant amount of contaminants can still be recognized. However, since we observed energetically unshifted single 1s core lines of the contributing elements (e.g., B 1s in h-BN: 190.7 eV) pointing to physisorbed rather than chemisorbed contaminants,[69] their influence on the electronic properties of the samples can be neglected.

III. RESULTS AND DISCUSSION

A. Valence-band properties

Figure 1 shows the valence-band spectra of the h-BN (a) and c-BN (b) films excited with monochromatized x rays (middle curves). The valence-band structure of the hexagonal BN film is dominated by two distinct features with maxima at about 12 and 20 eV, accompanied by a weak shoulder located at an energy of 26 eV. Obviously, the thin-film spectrum closely matches the experimental data taken from bulk h-BN [upper curve (Ref. 27)], proving the applicability of XPS measurements to *ex situ* prepared BN films.

By using x-rays to excite photoelectrons in a poly- or nanocrystalline sample, information about the density of

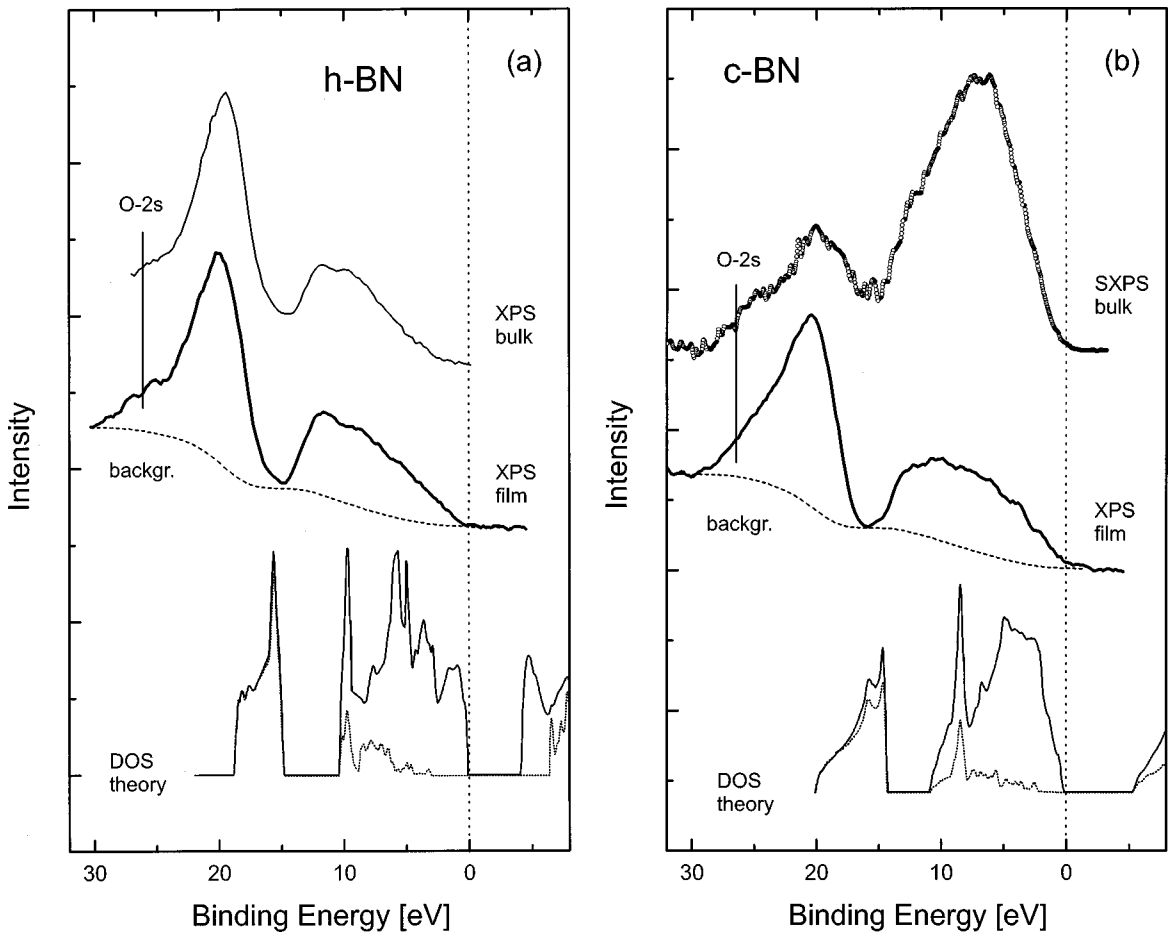

FIG. 1. (a) Valence-band spectrum of a h-BN thin film excited with monochromatized Al $K\alpha$ radiation ($h\nu = 1486.6$ eV, middle curve). The binding energy is referred to the Fermi level E_F as determined from a Au reference sample. The dotted line denotes the inelastically scattered background (Ref. 77). For comparison, experimental data from bulk material (Ref. 27) (upper curve) and calculated DOS results (Ref. 20) (lower curves: full line, total DOS; dotted line, partial s-DOS) are included; (b) XPS valence-band spectrum of a c-BN thin film (middle curve). For comparison, a photoelectron spectrum from bulk c-BN (Ref. 39) ($h\nu = 188.4$ eV, upper curve) and calculated DOS results (Ref. 20) (lower curves: full line, total DOS; dotted line, partial s-DOS) have been added.

states (DOS) of the material can be gained, since the momentum selection rules are averaged out.[70] Thus, an XPS spectrum taken from such a sample represents the sum of angular-momentum projected partial densities of states weighted by the corresponding photoionization cross sections. In the case of light elements with valence electrons of only s and p symmetry, the energy dependence of the cross sections[68] can advantageously be used to separate the two components. As in the case of graphite,[71] for photon energies in the keV range a preferential emission of electrons from the s-symmetric part of the BN valence band is expected.

Such a behavior can indeed be observed in Fig. 1(a), where our experimental results are compared with the total DOS and the s-symmetric part of the DOS as calculated[20,22] on the basis of first-principles local-density theory. Although good agreement is observed as far as band shapes are concerned, a striking difference exists for the corresponding bandwidths. In the XPS results, the bottom of the valence band is located at a binding energy of about 24 eV, which has to be compared with calculated values of 18 (Ref. 23) and 19 eV,[20] respectively.

According to Table I, carbon and oxygen contaminants amount to 4% each. As a result, a small shoulder at a binding energy of 26 eV is observed, which matches the energy position of the O 2s level. The necessarily connected emission from O 2p and C 2p states is suppressed for x-ray-induced transitions.[68] Emission from the C 2s level is reduced by a factor of 3 as compared to the O 2s state,[68] identifying the shoulder at 26 eV as the only relevant feature induced by contaminants. Hence, by applying XPS to an *ex situ* prepared h-BN film, valuable information about the s-symmetric states can be obtained, providing complementary information to the x-ray emission techniques, which are sensitive to the p-DOS in the boron-nitride system.

In the case of photoemission from the cubic phase, our data given in Fig. 1(b) represent the first x-ray-induced valence-band spectrum. Neither spectra from bulk material nor from thin films have been reported so far for c-BN. To allow a comparison, an electron-distribution curve is added instead, which has been acquired with photons in the soft x-ray regime from bulk material.[39] The XPS valence-band spectrum of the c-BN film exhibits a similar shape as found for the hexagonal phase. The increased intensity at 26 eV can be attributed to a higher amount of oxygen contaminations (see Table I).

While both experimental spectra in Fig. 1(b) are in accordance with respect to the energy positions of the two sub-

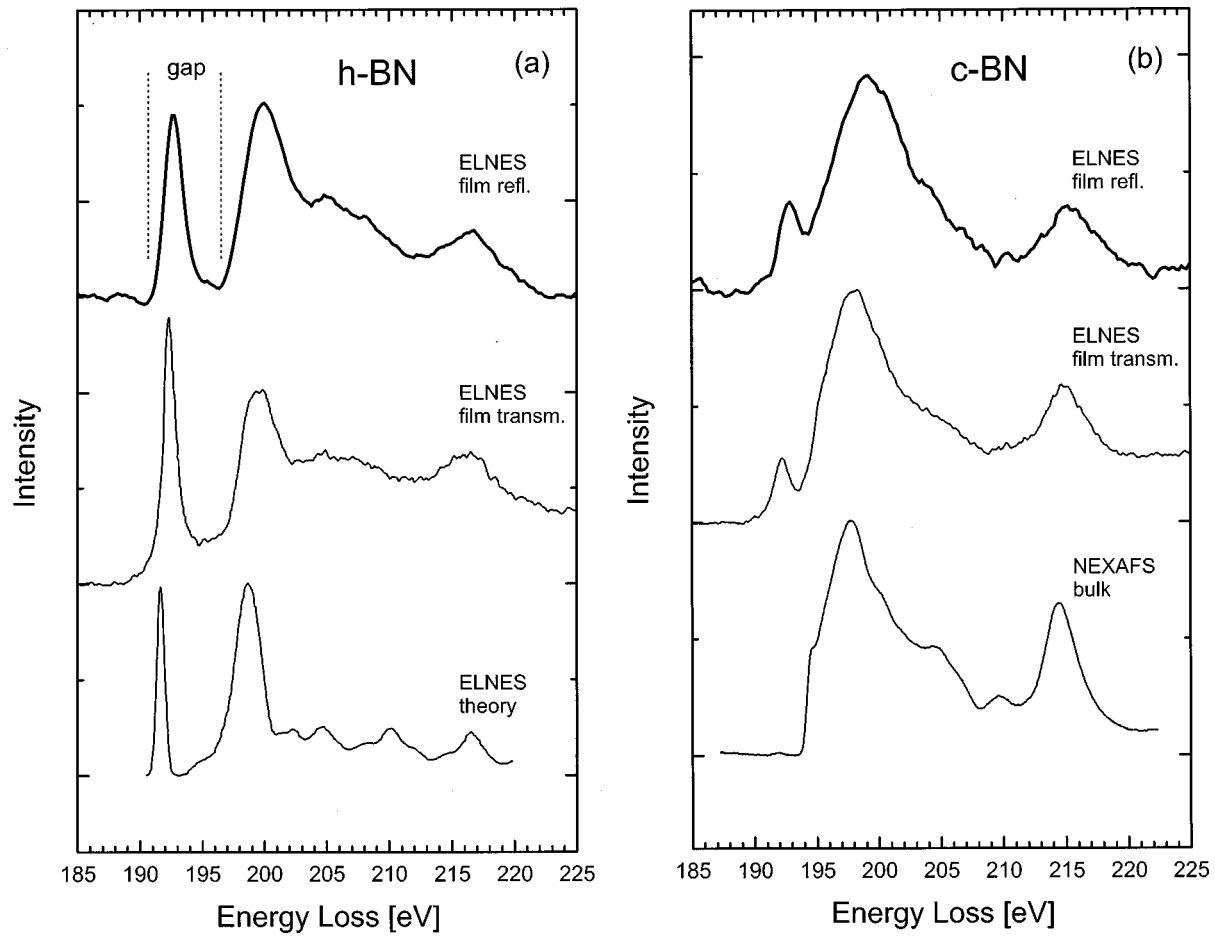

FIG. 2. (a) Comparison of ELNES results at the B *K*-edge for *h*-BN thin films: reflection geometry (upper curve, this paper); transmission geometry (Ref. 50) (middle curve); calculated spectrum (Ref. 23) (lower curve). (b) Comparison of ELNES spectra at the B *K*-edge for *c*-BN thin films: reflection geometry (upper curve, this paper); transmission geometry (Ref. 50) (middle curve); results as measured by core-level photoabsorption (NEXAFS) on bulk material (Ref. 45) (lower curve).

bands, a striking difference exists between the corresponding intensities. In the case of the lower excitation energy a much stronger emission is obtained in the low-binding-energy range, reflecting an enhanced photoemission from *p* states due to an increased photoionization cross section.[68] If we compare the experimental data with calculated densities of states,[20] the *s* contribution is again more suitable to interpret our XPS results. However, as in the case of the hexagonal phase, the total bandwidth as obtained from the experimental data is much larger than calculated, even if the influence of contaminants in the high-binding-energy range is taken into account.

Although valuable information can be obtained by XPS measurements about the distribution of occupied electronic states, the preferred sensitivity for *s*-symmetric states prevents a distinction of the hexagonal and cubic phases, which show their main differences in the *p*-derived states. Hence, complementary methods have to be applied, which will be presented in the next sections.

B. ELNES spectroscopy on the boron *K* edge

The energy loss of a primary electron beam due to excitations of 1*s* electrons into unoccupied states (*K* edges) has widely been used to study the volume electronic structure of BN samples thin enough to permit electron spectroscopy in the transmission mode (thickness 100 nm). The *K* edges of boron and nitrogen have also been studied extensively by photoabsorption (NEXAFS), a technique that also probes volume states in a sample.[72] The surface-sensitive method applied in this paper is based on the REELS technique, allowing us to use standard laboratory equipment to characterize energy losses due to B 1*s* core-level excitations.

The energy-loss fine structure within some 10 eV of the edge onset is known to reflect the site-projected local density of unoccupied electronic states.[73] In addition to ground-state electronic properties ELNES spectra may also reflect the existence of many-body effects as frequently observed for insulating materials. Sharp resonances do occur due to the transition of core electrons into localized final states (''core excitons''),[42,43] which are formed by the excited-core electron and the remaining core-hole state.

Figure 2(a) shows the boron *K*-edge ELNES spectrum of a hexagonal BN film, acquired with an electron beam of 1.7 keV primary energy incident under 50° to the sample surface (upper curve). The reflected electrons are detected in the normal direction. Since we are interested in the near-surface electronic structure and its correlation to the volume-electronic properties, data from an ELNES experiment performed in the transmission mode by McKenzie, Sainty, and

Green[50] and theoretical results by Ma *et al.*[23] for bulk material are included in the figure. Obviously, there is good overall agreement between the results of the different techniques allowing us to interpret the experimental findings along the theoretical results.

The most striking features in the ELNES spectrum of *h*-BN are given by a sharp peak at an energy loss of 192.3 eV, followed by additional structures at energy positions of about 200 and 217 eV, respectively. While the former is attributed to a bound exciton originating from the B $p_z(\pi^*)$ orbital, the latter are due to unoccupied $p_{xy}(\sigma^*)$ states.[23] Since π^* states are absent in the cubic phase due to sp^3 hybridization, the most significant peak in the REELS boron *K* edge at 192.3 eV can be used to identify the hexagonal phase, while the other features yield information about the unoccupied part of the electronic structure.

In order to verify the many-body character of the first peak in Fig. 2(a), we can take advantage of the XPS measurements introduced above. Using the energy position of the valence-band maximum [$E_B=0$, see Fig. 1(a)] with respect to the binding energy of the B 1*s* level ($E_B=190.65$ eV, see Fig. 5), the lower edge of the energy gap can be identified [Fig. 2(a), left line]. Taking an experimental value of 5.9 eV for the width of the energy gap in *h*-BN,[53] the upper edge of the gap can then be indicated (right line). Clearly, the energy position of the first peak is located within the energy gap of the hexagonal phase, identifying this feature as not belonging to the ground-state electronic structure but to represent an excitonic state.

Figure 2(b) shows the results of our surface-sensitive REELS measurements at the boron *K* edge for the *c*-BN film, together with data representing the volume properties[50] of a sample prepared by the same deposition technique. Since theoretical energy-loss data are not available for the cubic phase, a NEXAFS spectrum from bulk *c*-BN (Ref. 45) has been added for comparison. This time, the most prominent feature at an energy loss of 199 eV can be correlated with the density of states of the material, as can be done for the second major peak at 215 eV. In contrast to the expectations for sp^3 hybridized material, there still exists a peak at 192 eV in the electron-scattering experiments, which is nearly absent in the photon-induced spectrum of bulk material as recently confirmed.[49] Thus, the REELS results presented here clearly indicate the existence of a certain amount of *h*-BN being located in the near-surface part of the *c*-BN thin film.

This will be further investigated considering spectra taken at lower energy losses, where plasmon excitations can be studied.

C. Plasmon induced energy losses

The electron-loss function is intimately related to the complex dielectric function.[73] Hence, two different types of excitations may occur if a fast electron travels through the material to be investigated. First, interband transitions between occupied and unoccupied single-particle states may be excited corresponding to maxima in the imaginary part of the complex-dielectric function. Second, many-body resonances can occur due to zero crossings of the real part of the dielectric function, corresponding to volume and surface plasmons.

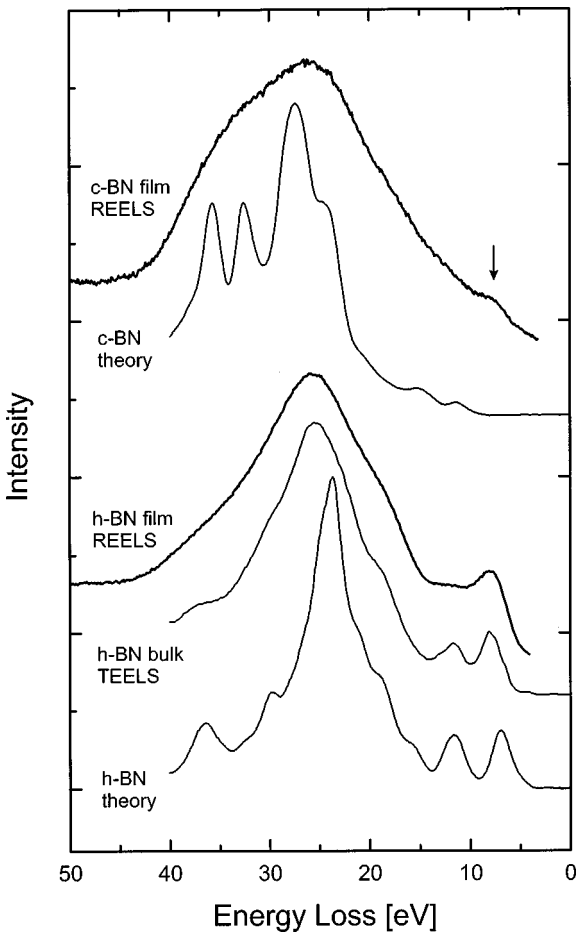

FIG. 3. Energy-loss function in the plasmon region for *h*-BN and *c*-BN films as compared to bulk material (Ref. 53) and to theory (Ref. 20). The spectrum assigned to bulk *h*-BN has been synthesized by averaging over the different directions in order to account for the nanocrystalline character of the thin film. The loss spectra of the films were corrected for background contributions (Ref. 78) for a better comparison with theory.

We will use both types of excitations to further characterize the near-surface electronic structure of our samples.

The energy-loss functions of *h*-BN and *c*-BN films are presented in Fig. 3, corrected for background contributions as described in Ref. 78. The REELS spectra have been obtained at a primary electron-beam energy of 2.5 keV, thus minimizing the contributions of surface plasmons. Analyzing the loss spectrum of the *h*-BN thin film (Fig. 3, lower part), two distinct features at energies of about 8 and 12 eV can be recognized. According to theory (lowest curve[20]), these features can be interpreted as originating from interband transitions between electronic states of π symmetry. Like the excitonic state, they can be used to identify the hexagonal phase.

The volume plasmon is located at 26 eV, which significantly differs from the value expected from theory (24 eV). In order to clarify this discrepancy, results derived from transmission experiments[53] on highly oriented *h*-BN are included. Good agreement is observed between the near-surface film and bulk-electronic properties of hexagonal boron nitride, although the width of the plasmon line is much larger in the thin-film loss spectrum compared to the bulk

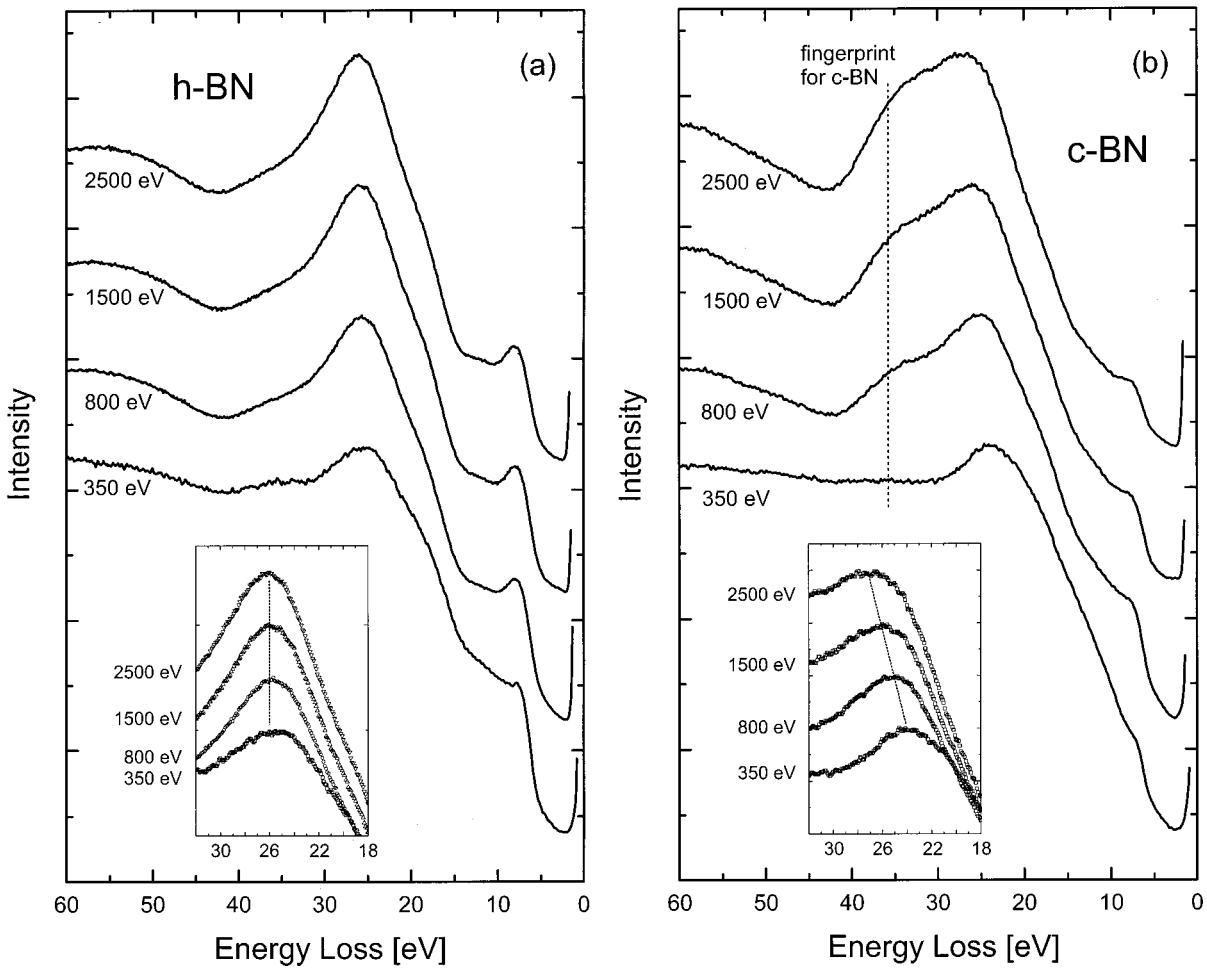

FIG. 4. REELS spectra of the h-BN (a) and c-BN (b) sample for various primary-electron energies. The insets show an enlarged view of the volume plasmon region.

material. Thus, fluctuations in the near-surface atomic structure of the film may be present leading to variations in the density and, therefore, in the plasmon energy. Again, the absolute energy positions of characteristic features are not well reproduced by theory.

The upper part of Fig. 3 shows our results for the c-BN film compared to the calculated spectrum.[20] According to theory, differences in the h-BN and c-BN loss functions should be visible as an increased plasmon energy in the cubic phase (reflecting the higher density), accompanied by the absence of π-π^* related features and the appearance of additional structures in the energy range between 30 and 40 eV. Though the details of these theoretically expected structures are smeared out, an increased intensity in this energy range can indeed be observed. Another important detail of the c-BN REELS spectrum is the small feature at low energy (shown by the arrow), which indicates that there is sp^2 related material still present in the film. This supports the findings of the previous section, where a π^*-induced excitonic state could still be observed in the c-BN data.

The spatial distribution of sp^2 bonded material can be analyzed taking advantage of the geometry of the experimental setup. In a REELS experiment, the information depth is determined by the electron mean free path of the primary as well as the inelastically scattered electrons. Adjusting the primary beam energy, therefore, offers the possibility to obtain a depth profile of the surface region. Based on our observations made above, no changes in the energy-loss function are expected for the h-BN sample, while for the c-BN sample strong variations should be visible in the loss spectrum in case of an inhomogeneous distribution normal to the surface, which has previously been suggested by several authors.[55,57,62,63]

REELS spectra for a decreasing electron-beam energy E_0 are shown in Fig. 4. For the hexagonal film [Fig. 4(a)], only minor variations are detected from the top to the bottom curve as far as the plasmon energy and the general shape of the loss function are concerned. Owing to the increasing surface sensitivity with lowering E_0, the surface-plasmon contribution gains in intensity, being identified as a shoulder at an energy loss of about 17 eV. In contrast to Fig. 4(a), drastic changes are visible for the cubic specimen in Fig. 4(b). For decreasing information depth, the feature characteristic of the cubic phase located at energies >30 eV nearly vanishes, leaving a single maximum at a significantly reduced energy [Fig. 4(b), inset] as it is typical of h-BN. These results unambiguously reflect the presence of a sp^2 bound-surface layer, which terminates the cubic film. This strongly supports the observation that c-BN films in general are covered by an h-BN-like ultrathin film,[57,63] which is stable under ambient conditions as seen in the present investigation.

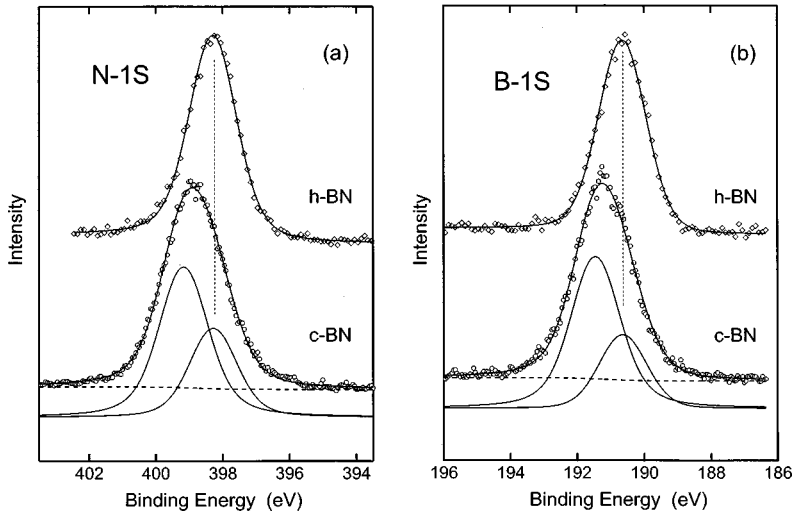

FIG. 5. XPS photoemission spectrum of the N 1*s* (a) and the B 1*s* (b) core level in hexagonal (upper curves) and cubic (lower curves) boron nitride thin films. The full lines indicate the result of a least-squares fitting procedure (Ref. 67) using Doniach-Sunjic line shapes with the asymmetry parameter constrained to zero to account for the insulating character of the samples. The lower two spectra are fitted with two components, representing the contribution of the hexagonal and the cubic phase, respectively.

The chemical state of the probed volume will now be analyzed in more detail, allowing us to proceed one step beyond the analysis performed so far. Taking advantage of the capability of core-level spectroscopy to distinguish between different atomic arrangements we will be able to determine the thickness of the sp^2-bound surface layer.

D. Core-level spectroscopy

Examining the core levels of the constituents, we can deduce additional information about a material to be studied, since core-level binding energies are closely related to the local chemical and topological environment of the probed atoms. Changes in the valence-band structure due to bonding are usually reflected in distinct binding-energy shifts of core electrons with respect to the pure material, known as the ''chemical shift.'' XPS spectra are presented in Fig. 5 for the N 1*s* [Fig. 5(a)] and the B 1*s* [Fig. 5(b)] core level, which have been excited with monochromatized Al $K\alpha$ radiation.

All core-level spectra were analyzed applying a numerical least-squares fitting procedure[67] using Doniach-Sunjic line shapes.[74] In order to account for the insulating character of the material, the asymmetry parameter has been constrained to zero (symmetric lines) in each case. As can be seen from the upper two curves in Fig. 5, single lines are sufficient to obtain good fits for the *h*-BN film. This is consistent with the observations from the previous sections, which indicated a single *h*-BN phase having bulk character. For the *c*-BN film, a second component has to be included in order to achieve a reliable fit.

Based on the observation of a *h*-BN-like surface layer terminating the cubic phase, the properties of the buried cubic material can be extracted by adjusting the line-shape parameters of one of the components to the corresponding values deduced from the hexagonal phase. This leads to differences in binding energy between both crystal structures of 0.82 eV for the B 1*s* and 0.89 eV for the N 1*s* line, respectively. Since photoelectrons emitted from the buried layer are damped in the top layer according to their inelastic mean free path[75] in the hexagonal phase, the integrated intensities of the different components can be used to determine the thickness of the top layer. This procedure yields values of 0.87 nm for the photoemission of B 1*s* electrons and, independently, 0.92 nm for the emission from N 1*s* states. These values are in good agreement with earlier estimates for films analyzed *in situ*.[40,57] Obviously, a 3-monolayer-thick film of *h*-BN-like material on top of *c*-BN is structurally and chemically stable even under ambient conditions.

E. Influence of ion bombardment

Ion bombardment during thin-film growth is essential to promote the formation of the cubic phase. Consequently, defects induced by the irradiation process are expected to have a strong influence on both the atomic and electronic properties. Recently, it has been demonstrated[57] that increasing the degree of disorder by post-irradiation of *c*-BN films with ions induces significant energy shifts of the plasmon-loss line. The widely varying values reported in literature may, therefore, be attributed to variations in the overall degree of disorder during film preparation. Defects, on the other hand, are known to influence core-excitonic states as observed in NEXAFS experiments.[47,49]

In Fig. 6 ELNES spectra from the B *K*-edge region are presented for *c*-BN and *h*-BN films after annealing to 520 K (upper two curves) and after *in situ* postirradiation with 5 keV Ar^+ ions (10^{16} ions/cm^2, lower two curves), sufficient to achieve equilibrium conditions in the near-surface part of the samples. The calculated damage profile using the Monte Carlo code TRIM (Ref. 76) extends to a depth of about 5 nm a value exceeding the sampling depth of the spectroscopy.

While for the annealed films distinct differences can be recognized for, e.g., the onset of the σ^* bands or, especially, for the intensity of the excitonic state being a fingerprint for *h*-BN the spectra of the irradiated samples are very similar. After ion irradiation, both samples exhibit a very intense

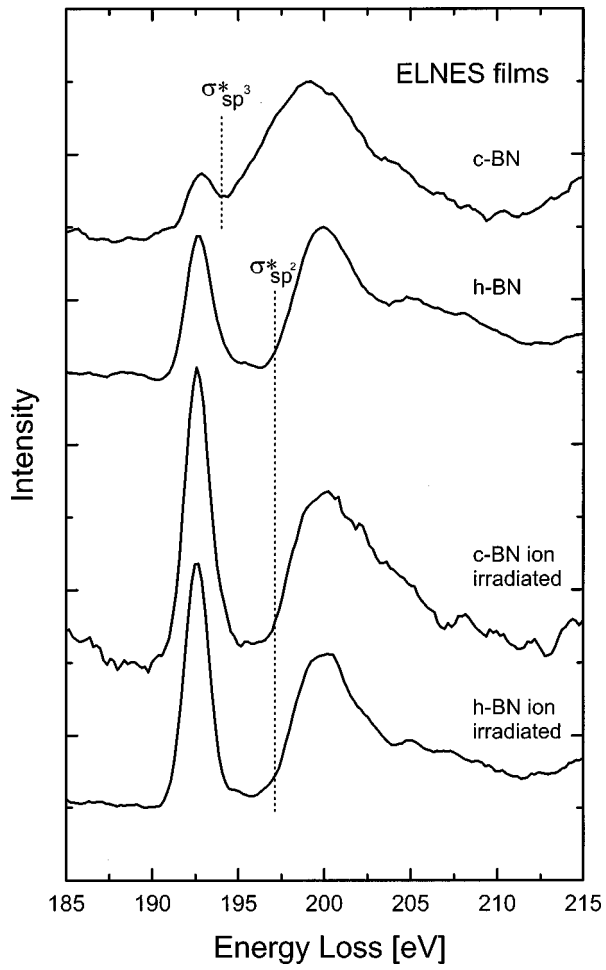

FIG. 6. Comparison of ELNES spectra from the B *K*-edge region for *ex situ* prepared boron nitride thin films: after annealing to 520 K (upper two curves); after postirradiation with 5 keV Ar^+ ions with a fluence of $10^{16}/cm^2$ (lower two curves).

excitonic state at 192 eV, and an onset of the σ^* band which, shifted to higher energies, is in agreement with the position observed for the *h*-BN phase. Obviously, the cubic phase has been transformed within the probed volume into a *h*-BN-like material. But even for the *h*-BN thin film, with very similar shapes of the unoccupied density of states before and after ion bombardment, a significant increase in intensity is detectable for the excitonic signal. This is consistent with NEXAFS experiments[47] on thin films and bulk powders, where an increased intensity for void-induced exciton lines has been found under ion bombardment.

Additional REELS measurements taken in the plasmon energy range of both types of irradiated films confirm the observed changes. They also result in almost identical spectra reflecting the properties of *h*-BN-like material.

IV. CONCLUSIONS

In conclusion, we have demonstrated the capability of electron spectroscopy to reliably characterize *ex situ* prepared hexagonal and cubic boron nitride thin films. By combining surface-sensitive techniques like x-ray photoelectron spectroscopy with reflection electron-energy-loss spectroscopy in both the plasmon as well as the *K*-edge region, ground-state properties and many-body phenomena can be studied. This allows us to extract information about the bulk electronic structure for both the occupied and unoccupied electronic states. While general agreement is observed between theory and experiment for *h*-BN films as far as band shapes are concerned, there still exists the problem of bandwidths being underestimated by theory. In the case of *c*-BN films prepared by ion-beam-assisted sputter deposition, though the general situation is similar, a *h*-BN-like surface layer can be identified, whose thickness can be determined to a value of 0.9 nm. Low-energy ion bombardment is found to significantly increase the amount of near-surface disorder, leading to the transformation of *c*-BN into a *h*-BN-like material.

ACKNOWLEDGMENTS

We thank Professor Dr. J. Fink (Dresden) for valuable suggestions. Financial support by the Deutsche Forschungsgemeinschaft (DFG), the trinational D-A-CH cooperation on the synthesis of superhard coatings, and Schweizer Nationalfonds (NF) is gratefully acknowledged.

[1] T. K. Pauli, P. Bhattacharya, and D. N. Bose, Appl. Phys. Lett. **56**, 2648 (1990).
[2] S. S. Dana, Mater. Sci. Forum **54/55**, 229 (1990).
[3] K. Miyoshi, D. H. Buckley, J. J. Pouch, S. A. Alterovitz, and H. E. Sliney, Surf. Coat. Technol. **33**, 221 (1987).
[4] L. Vel, G. Demazeau, and J. Etourneau, Mater. Sci. Eng., B **10**, 149 (1991).
[5] R. W. Pryor, Appl. Phys. Lett. **68**, 1802 (1996).
[6] M. J. Powers, M. C. Benjamin, L. M. Porter, R. J. Nemanich, R. F. Davis, J. J. Cuomo, G. L. Doll, and S. J. Harris, Appl. Phys. Lett. **67**, 3912 (1995).
[7] L. Kleinmann and J. C. Phillips, Phys. Rev. **117**, 460 (1960).
[8] A. Zunger and A. J. Freeman, Phys. Rev. B **17**, 2030 (1978).
[9] Y. F. Tsay, A. Vaidyanathan, and S. S. Mistra, Phys. Rev. B **19**, 5422 (1979).
[10] R. Dovesi, C. Pisani, C. Roetti, and P. Dellarole, Phys. Rev. B **24**, 4170 (1981).
[11] C. Prasad and J. D. Dubey, Phys. Status Solidi B **125**, 629 (1984).
[12] M. Z. Huang and W. Y. Ching, J. Phys. Chem. Solids **46**, 977 (1985).
[13] R. M. Wentzcovitch, K. J. Chang, and M. L. Cohen, Phys. Rev. B **34**, 1071 (1986).
[14] K. T. Park, K. Terakura, and N. Hamada, J. Phys. C **20**, 1241 (1987).
[15] R. M. Wentzcovitch, S. Fahy, M. L. Cohen, and S. G. Louie, Phys. Rev. B **38**, 6191 (1988).
[16] P. E. van Camp, V. E. van Doren, and J. T. Devreese, Phys. Status Solidi B **146**, 573 (1988).
[17] P. E. van Camp, V. E. van Doren, and J. T. Devreese, Solid State Commun. **71**, 1055 (1989).

[18] E. K. Takahashi, A. T. Lino, A. C. Ferraz, and J. R. Leite, Phys. Rev. B **41**, 1691 (1990).
[19] M. P. Surh, S. G. Louie, and M. L. Cohen, Phys. Rev. B **43**, 9126 (1991).
[20] Y.-N. Xu and W. Y. Ching, Phys. Rev. B **44**, 7787 (1991).
[21] K. Kikuchi, T. Usa, A. Sakuma, M. Hiraro, and Y. Murayama, Solid State Commun. **81**, 653 (1992).
[22] Y. N. Xu and W. Y. Ching, Phys. Rev. B **48**, 4335 (1993).
[23] H. Ma, S. H. Lin, R. W. Carpenter, P. Rice, and O. F. Sankey, J. Appl. Phys. **73**, 7422 (1993).
[24] V. V. Ilyasov, I. Y. Nikiforov, and N. Y. Safontseva, Phys. Status Solidi B **185**, 171 (1994).
[25] I. Y. Nikiforov, V. V. Ilyasov, and N. Y. Safontseva, J. Phys.: Condens. Matter **7**, 6035 (1995).
[26] V. A. Fomichev and M. A. Rumsh, J. Phys. Chem. Solids **29**, 1015 (1968).
[27] E. Tegeler, N. Kosuch, G. Wiech, and A. Faessler, Phys. Status Solidi B **91**, 223 (1979).
[28] R. D. Carson and S. E. Schnatterly, Phys. Rev. Lett. **59**, 319 (1987).
[29] A. Mansour and S. E. Schnatterly, Phys. Rev. B **36**, 9234 (1987).
[30] S. Luck and D. S. Urch, Phys. Scr. **41**, 970 (1990).
[31] W. L. O'Brien, J. Jia, Q. Y. Dong, T. A. Callcott, K. E. Miyano, D. L. Ederer, D. R. Mueller, and C. C. Kao, Phys. Rev. Lett. **70**, 238 (1993).
[32] Y. Muramatsu, M. Oshima, J. Kawai, S. Tadekoro, H. Adachi, A. Agui, S. Shin, H. Kato, H. Kohsuki, and M. Motoyama, Phys. Rev. Lett. **76**, 3846 (1996).
[33] J. J. Jia, T. A. Callcott, E. L. Shirley, J. A. Carlisle, L. J. Terminello, A. Asfaw, D. L. Ederer, F. J. Himpsel, and R. C. C. Perera, Phys. Rev. Lett. **76**, 4054 (1996).
[34] A. Agui, S. Shin, M. Fujisawa, Y. Tezuka, T. Ishii, Y. Muramatsu, O. Mishima, and K. Era, Phys. Rev. B **55**, 2073 (1997).
[35] Y. Muramatsu, H. Kouzuki, T. Kaneyoshi, M. Motoyama, A. Agui, S. Shin, H. Kato, and J. Kawai, Appl. Phys. A: Mater. Sci. Process. **65**, 191 (1997).
[36] J. Barth, C. Kunz, and T. M. Zimkina, Solid State Commun. **36**, 453 (1980).
[37] R. Trehan, Y. Lifshitz, and J. W. Rabalais, J. Vac. Sci. Technol. A **8**, 4026 (1990).
[38] J. P. Riviere, Y. Pacaud, and M. Cahoreau, Thin Solid Films **227**, 44 (1993).
[39] S. Shin, A. Agui, M. Fujisawa, Y. Tezuka, T. Ishii, Y. Minagawa, Y. Suda, A. Ebina, O. Mishima, and K. Era, Phys. Rev. B **52**, 11 853 (1995).
[40] K. S. Park, D. Y. Lee, K. J. Kim, and D. W. Moon, J. Vac. Sci. Technol. A **15**, 1041 (1997).
[41] C. Oshima and A. Nagashima, J. Phys.: Condens. Matter **9**, 1 (1997).
[42] F. C. Brown, R. Z. Bachrach, and M. Skibowski, Phys. Rev. B **13**, 2633 (1976).
[43] B. M. Davies, F. Bassani, and F. C. Brown, Phys. Rev. B **24**, 3537 (1981).
[44] D. R. Strongin, J. K. Mowlem, M. W. Ruckman, and M. Strongin, Appl. Phys. Lett. **60**, 2561 (1992).
[45] A. Chaiken, L. J. Terminello, J. Wong, G. L. Doll, and C. A. Taylor II, Appl. Phys. Lett. **63**, 2112 (1993).
[46] J. Moscovici, G. Loupias, P. Parent, and G. Tourillon, J. Phys. Chem. Solids **57**, 6 (1996).
[47] I. Jiménez, A. F. Jankowski, L. J. Terminello, J. A. Carlisle, D. G. J. Sutherland, G. L. Doll, J. V. Mantese, W. M. Tong, D. K. Shuh, and F. J. Himpsel, Appl. Phys. Lett. **68**, 2816 (1996).
[48] D. H. Berns, M. A. Cappelli, and D. K. Shuh, Diamond Relat. Mater. **6**, 1883 (1997).
[49] I. Jiménez, A. F. Jankowski, L. J. Terminello, J. A. Carlisle, D. G. J. Sutherland, G. L. Doll, J. V. Mantese, W. M. Tong, D. K. Shuh, and F. J. Himpsel, Phys. Rev. B **55**, 12 025 (1997).
[50] D. R. McKenzie, W. G. Sainty, and D. Green, Mater. Sci. Forum **54/55**, 193 (1990).
[51] T. Hayashi, K. Araki, S. Takatoh, T. Enokijima, T. Yikegaki, T. Futami, Y. Kurihara, J. Tsukajima, K. Takamoto, T. Fujikawa, and S. Usami, Appl. Phys. Lett. **66**, 25 (1995).
[52] U. Büchner, Phys. Status Solidi B **81**, 227 (1977).
[53] C. Tarrio and S. E. Schnatterly, Phys. Rev. B **40**, 7852 (1989).
[54] H. Chen, Y. He, and R. H. Prince, Diamond Relat. Mater. **5**, 552 (1996).
[55] G. Sene, D. Bouchier, S. Ilias, M. A. Djouadi, J. Pascallon, V. Stambouli, P. Moller, and G. Hug, Diamond Relat. Mater. **5**, 530 (1996).
[56] M. F. Plass, W. Fukarek, A. Kolitsch, and W. Möller, Diamond Relat. Mater. **6**, 5 (1997).
[57] P. Widmayer, P. Ziemann, and H.-G. Boyen, Diamond Relat. Mater. **7**, 385 (1998).
[58] S. Ilias, V. Stambouli, J. Pascallon, D. Bouchier, and G. Nouet, Diamond Relat. Mater. **7**, 389 (1998).
[59] K. P. Loh, I. Sakaguchi, M. Nishitani-Gamo, T. Taniguchi, and T. Ando, Phys. Rev. B **56**, R12 791 (1997).
[60] M. Z. Karim, D. C. Cameron, and M. S. J. Hashmi, Mater. Des. **13**, 207 (1992).
[61] T. Yoshida, Diamond Relat. Mater. **5**, 501 (1996).
[62] K. S. Park and D. Y. Lee, Appl. Phys. Lett. **70**, 315 (1997).
[63] M. F. Plass, W. Fukarek, A. Kolitsch, N. Schell, and W. Möller, Thin Solid Films **305**, 172 (1997).
[64] D. R. McKenzie, D. J. H. Cockayne, D. A. Muller, M. Murakawa, S. Miyake, S. Watanabe, and P. Fallon, J. Appl. Phys. **70**, 3007 (1991).
[65] T. A. Friedmann, P. B. Mirkarimi, D. L. Medlin, K. F. McCarty, E. J. Klaus, D. R. Boehme, H. A. Johnsen, M. J. Mills, D. K. Ottesen, and J. C. Barbour, J. Appl. Phys. **76**, 3088 (1994).
[66] Z. Wei-Lei, Y. Ikuhara, M. Murakawa, S. Watanabe, and T. Suzuki, Appl. Phys. Lett. **66**, 2490 (1995).
[67] G. K. Wertheim and S. B. Dicenzo, J. Electron Spectrosc. Relat. Phenom. **37**, 57 (1985).
[68] J. Yeh and I. Lindau, At. Data Nucl. Data Tables **32**, 1 (1985).
[69] C. D. Wagner, W. M. Riggs, L. E. Davis, J. F. Moulder, and G. E. Muilberg, *Handbook of X-ray Photoelectron Spectroscopy* (Perkin Elmer, Eden Prairie, MN, 1979).
[70] S. Hüfner, in *Photoelectron Spectroscopy*, edited by M. Cardona, Springer Series in Solid State Science Vol. 82 (Springer, Berlin, 1995), p. 355.
[71] A. Bianconi, S. B. M. Hagström, and R. Z. Bachrach, Phys. Rev. B **16**, 5543 (1977).
[72] D. G. Sutherland, H. Akatsu, M. Copel, F. J. Himpsel, T. A. Callcot, J. A. Carlisle, D. L. Ederer, J. J. Jia, I. Jimenez, R. Perera, D. K. Shuh, L. J. Terminello, and W. M. Tong, J. Appl. Phys. **78**, 6761 (1995).
[73] J. Fink, Adv. Electron. Electron Phys. **75**, 121 (1989).
[74] S. Doniach and M. Sunjic, J. Phys. C **3**, 385 (1970).
[75] S. Tanuma, C. J. Powell, and D. R. Penn, Surf. Sci. **192**, L849 (1987).
[76] J. P. Biersack and L. G. Haggmark, Nucl. Instrum. Methods **174**, 257 (1989).
[77] D. A. Shirley, Phys. Rev. B **5**, 4709 (1972).
[78] S. Tougaard and J. Kraaer, Phys. Rev. B **43**, 1651 (1991).